Electrochimica Acta 139 (2014) 104–110

Contents lists available at ScienceDirect

Electrochimica Acta

journal homepage: www.elsevier.com/locate/electacta

AlF_3 modification to suppress the gas generation of $Li_4Ti_5O_{12}$ anode battery

Wen Li[a,b], Xing Li[c,*], Mianzhong Chen[a], Zhengwei Xie[a,b], Jingxian Zhang[a,b], Shaoqiang Dong[a,b], Meizhen Qu[a,*]

[a] Chengdu Institute of Organic Chemistry, Chinese Academy of Sciences, Chengdu 610041, PR China
[b] Graduate University of Chinese Academy of Sciences, Beijing 100039, PR China
[c] School of Materials Science and Engineering, Southwest Petroleum University, Chengdu 610500, PR China

ARTICLE INFO

Article history:
Received 27 May 2014
Received in revised form 2 July 2014
Accepted 9 July 2014
Available online 16 July 2014

Keywords:
$Li_4Ti_5O_{12}$
AlF_3-modified
Layer
Suppress
Gas generation

ABSTRACT

Commercial $Li_4Ti_5O_{12}$ is modified by AlF_3 with the purpose of suppressing the gas generation of $Li_4Ti_5O_{12}$ anode battery. The prepared AlF_3-modified $Li_4Ti_5O_{12}$ is characterized by a variety of means such as X-ray diffraction, scanning electron microscope, transmission electron microscope and X-ray photoelectron spectroscopy. The results indicate that only part of Al^{3+} and F^- have co-doped into the bulk phase of $Li_4Ti_5O_{12}$ particles, while the rest of the Al^{3+} and F^- remain on the surface of the $Li_4Ti_5O_{12}$ particles to form an AlF_3 coating layer. The AlF_3 coating layer on the surface of AlF_3-modified $Li_4Ti_5O_{12}$ is very effective in suppressing the gas generation of $Li_4Ti_5O_{12}$ anode battery. AlF_3 modification is a simple yet very effective strategy, which can both improve the high-rate charge/discharge performance of $Li_4Ti_5O_{12}$ and suppress the gassing behavior of $Li_4Ti_5O_{12}$ anode battery.

1. Introduction

Spinel $Li_4Ti_5O_{12}$ (LTO) possesses zero volume change during charge/discharge processes, high working potential of the redox couple Ti^{4+}/Ti^{3+} (ca. 1.55 V vs. Li/Li^+), excellent safety and thermal stability, and long cycle life in a wide operating temperature range [1–3]. Therefore, it has been considered to be a promising alternative to graphite anode materials for large-scale lithium-ion batteries application in electric vehicles and hybrid electric vehicles [4–6].

Unfortunately, LTO shows a low intrinsic electrical conductivity and a moderate lithium-ion diffusion coefficient, which seriously hinder its high-rate performance [7]. To overcome these problems, a number of approaches, e.g., constructing nanostructured LTO [8–11], doping cations and anions such as Al^{3+} [12–14], Mg^{2+} [15], Zr^{4+} [16,17], Zn^{2+} [18], Mo^{6+} [19], La^{3+} [20], V^{5+} [21], Nb^{5+} [22], Mn^{4+} [23] and Br^- [24] into LTO, and introducing carbon [25–27], metal [28] or metal oxide into LTO [29–31], have been widely used to improve the electrochemical performance of LTO anodes. Even after a variety of efforts based on the above strategies, LTO anode is still not considered as the most preferable choice for large-scale applications in power LIB industries. This is because the LIBs using LTO as anode material are easily inflated during charge/discharge cycles, especially at elevated temperature condition [32,33]. So far, there are only a few reports that specifically refer to the gassing behavior of LTO electrodes [32–36]. Very recently, the carbon coating is demonstrated to be an effective strategy, which can both improve the high-rate charge/discharge performance of batteries and suppress the gassing behavior of LTO anode battery [37]. The carbon layer could control the interfacial reactions between LTO and the surrounding electrolyte solution effectively, thereby suppressing the gassing of LTO anode battery [37]. The carbon coating process is usually carried at a high temperature (600 ~ 800 °C), which might easily cause the reaction between carbon and LTO, thereby changing the surface structure of LTO associated with the capacity decrease. In addition, the existence of carbon coating is likely to be a threat to the safety of batteries. Therefore, low temperature and safe coating layer should be proposed during the modified process.

To the best of our knowledge, AlF_3 has been widely used to modify the surface of cathode materials [38–42] and graphite [43] via a low-temperature (400 °C) reaction approach. The improved electrochemical performance was tentatively attributed to the "buffer" layer provided by the AlF_3 coating, which reduced the activity of the extracted oxygen and suppressed the electrolyte decomposition [40]. Recently, the commercial LTO was also successfully modified

* Corresponding author. Chengdu Institute of Organic Chemistry, Chinese Academy of Sciences, Chengdu 610041, PR China. Tel.: +86 28 85229790; fax: +86 28 85242280.
E-mail addresses: lixing@swpu.edu.cn (X. Li), mzhqu@cioc.ac.cn (M. Qu).

http://dx.doi.org/10.1016/j.electacta.2014.07.017
0013-4686/

by AlF_3 via the same process as mentioned above, and the AlF_3-modified LTO has ultrahigh rate capability as compared with the commercial LTO [44]. In the above work, it was suggested that all the Al^{3+} and F^- are co-doped into the LTO particles to form a composite material that mainly consists of Al^{3+} and F^- co-doped LTO and a small amount of anatase TiO_2. The reason for the improvement of electrochemical performance has been explained as that the in-situ generated TiO_2 limited the growth of LTO particles, leading to higher surface area or higher exchange current density and providing short ionic diffusion path through the boundary among TiO_2 and LTO.

In the present work, we modified the commercial LTO using AlF_3 with the purpose of suppressing gassing in LTO anode batteries. The AlF_3-modified LTO also achieved higher specific capacity and rate capability than that of the commercial LTO. We found for the first time that only part of the Al^{3+} and F^- are co-doped into the bulk phase of the LTO particles, while the rest of the Al^{3+} and F^- remain on the surface of the LTO particles to form a thin AlF_3 coating layer, through studying the characteristics of the AlF_3-modified LTO. We suggest that the AlF_3 coating layer on the surface of AlF_3-modified LTO is likely to suppress the electrolyte decomposition, thereby preventing the gas generation of LTO anode batteries.

2. Experimental

2.1. Materials synthesis

The AlF_3-modified LTO samples were prepared following the process described by Xu [38]. Commercial LTO (Chengdu Xingneng New Materials Co., LTD) powders were used for this study. Ammonium fluoride (NH_4F, 98%, Sigma-Aldrich) and aluminum nitrate nonahydrate ($Al(NO_3)_3.9H_2O$, 98%, Sigma-Aldrich) were added at a fixed stoichiometric molar ratio of $Al^{3+}/F^- = 1/3$, and the weight ratio of AlF_3/LTO is 2 wt.%. After being constantly stirred at 80 °C for 5 h and filtration, the solid powder was calcined at 400 °C for 5 h under argon atmosphere.

2.2. Materials characterization

Powder X-ray diffraction (XRD, Xpert MPD DY1219) with Cu Kα radiation was used to identify the phase composition and crystal lattice parameters of all the LTO samples. The diffraction patterns were collected at room temperature by step scanning in the range of 10 ~ 90° at a scanning rate of 0.02° per 10 s. The particle size and particulate morphology were examined by scanning electron microscope (SEM, INCA Penta FETx3) and transmission electron microscope (TEM, JEOL JEM-2010F). The chemical composition of the LTO sample was determined by X-ray photoelectron spectroscopy (XPS, PHI5600 Physical Electronics).

2.3. Coin-type half cells electrochemical measurements

The working electrode was prepared by mixing 85 wt.% active material (pure LTO or AlF_3-modified LTO), 10 wt.% conductive Super-P and 5 wt.% LA-132 binder into a slurry, and coating the slurry on an alumina foil by painting. Afterwards, the working electrode was dried in a vacuum oven at 105 °C for 12 h to remove any residual solvent and possible adsorbed moisture. Electrochemical measurements were performed using coin-type half cells assembled in an argon-filled glove box. The cell consisted of the as-prepared working electrode, microporous polypropylene membrane (Celgard 2400, Celgard Inc., USA) as separator and lithium foil as counter electrode. The electrolyte was 1 M $LiPF_6$ solution in ethylene carbonate (EC): diethyl carbonate (DEC): ethyl methyl carbonate (EMC) with a volume ratio of 1:1:1.

Galvanostatic charge and discharge experiments were carried out on an automatic galvanostatic charge/discharge unit (Land CT 2001A, Wuhan, China) between 1.0 and 3.0 V at different charge/discharge rates at 25 °C. Cyclic voltammertry (CV) and electrochemical impedance spectroscopy (EIS) tests were conducted on an electrochemical workstation (PARSTAT 2273). In the case of CVs, the potential range was set from 1.0 to 3.0 V while the scan rate was set at 0.1 mV s^{-1}. EIS tests were operated with an alternating

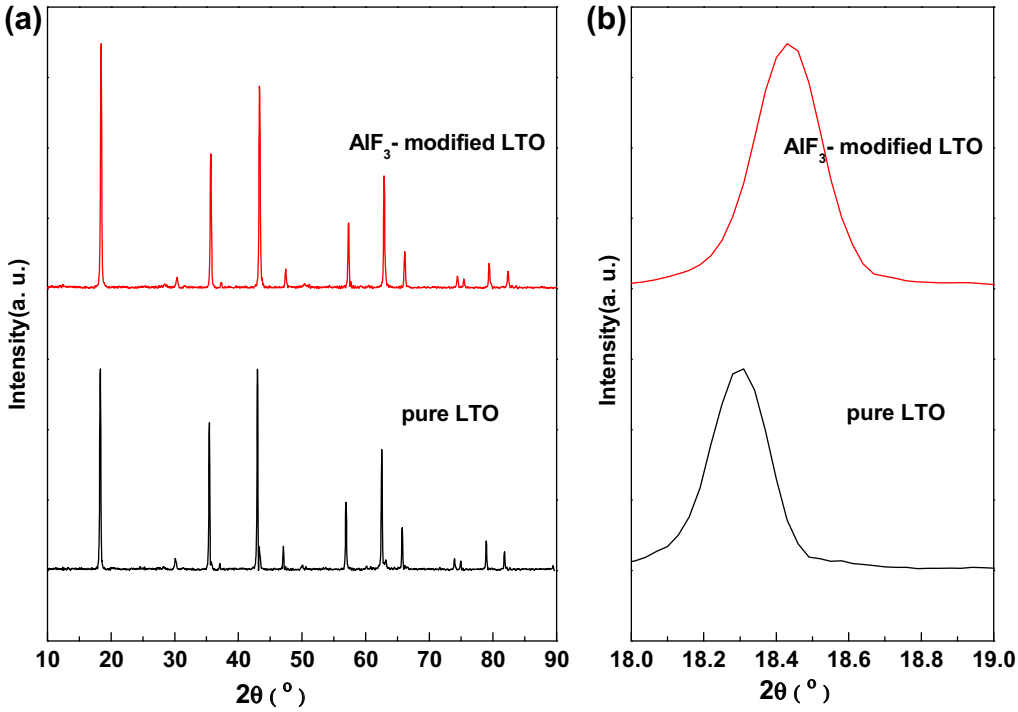

Fig. 1. (a) XRD patterns and (b) enlarged peaks at $2\theta = 18.0° \sim 19.0°$ of pure LTO and AlF_3-modified LTO.

current voltage in the frequency range of 10 mHz to 100 kHz at the first cycle and half charged state.

2.4. Gassing behaviors of soft-packed LMO/LTO batteries

Custom 2645110 type soft-packed LMO/LTO batteries, of 2.6 mm thick, 45 mm wide and 110 mm long, were assembled to investigate the gassing behaviors of LTO. The batteries were made of $LiMn_2O_4$ (LMO) (Yunnan Huilong Group Co., LTD) as the cathode, commercial LTO or AlF_3-modified LTO as the anode, microporous polypropylene membrane (Celgard 2400, Celgard Inc., USA) as the separator, and 1 M $LiPF_6$ solution in EC: DEC: EMC with a volume ratio of 1:1:1 as the electrolyte. The LMO cathode consisted of 93 wt.% LMO, 4 wt.% Super-P and 3 wt.% LA-132 binder, whereas the LTO anode consisted of 87 wt.% commercial LTO or AlF_3-modified LTO, 7 wt.% Super-P and 6 wt.% LA-132. These components were rolled together to form the battery core and assembled into aluminum-plastic laminated film packages. Batteries were charged and discharged once between 1.0 and 3.0 V at a rate of 0.2 C (1 C =600 mAh) for stabilization before cyclic tests, then charged and discharged 300 cycles between 1.3 and 2.8 V at a rate of 1 C at 25 °C.

3. Results and discussion

The XRD patterns of the pure LTO and AlF_3-modified LTO are shown in Fig. 1a. The patterns of both samples are in good agreement with JCPDS file of standard spinel LTO (card No. 49-0207).

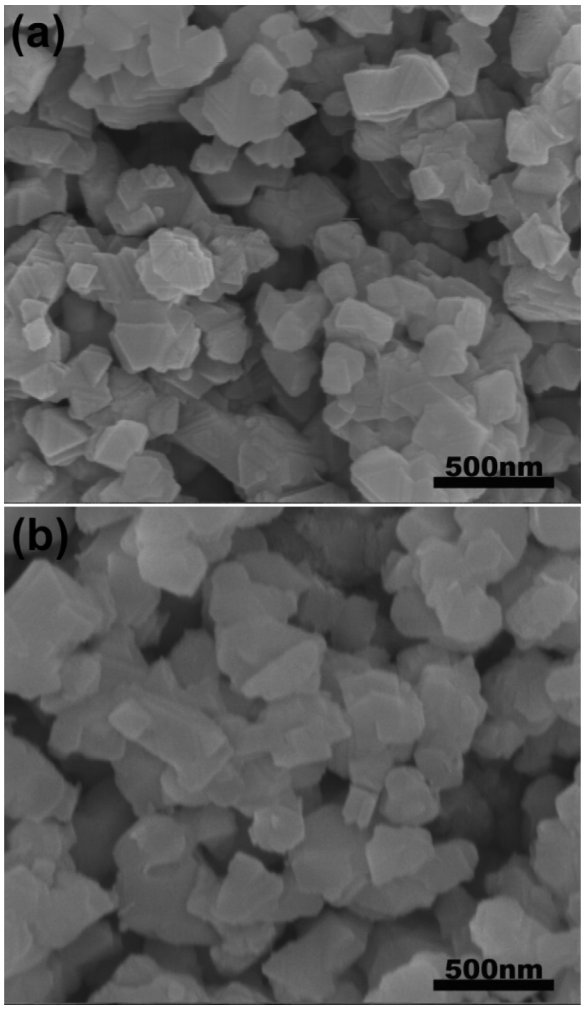

Fig. 2. SEM images of (a) pure LTO and (b) AlF_3-modified LTO.

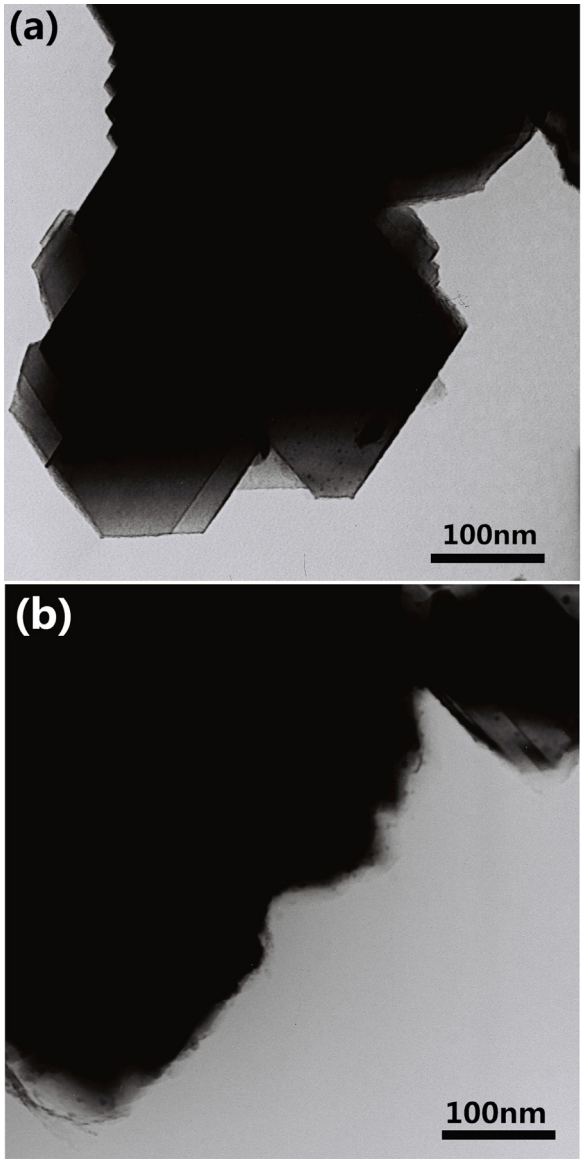

Fig. 3. TEM images of (a) pure LTO and (b) AlF_3-modified LTO.

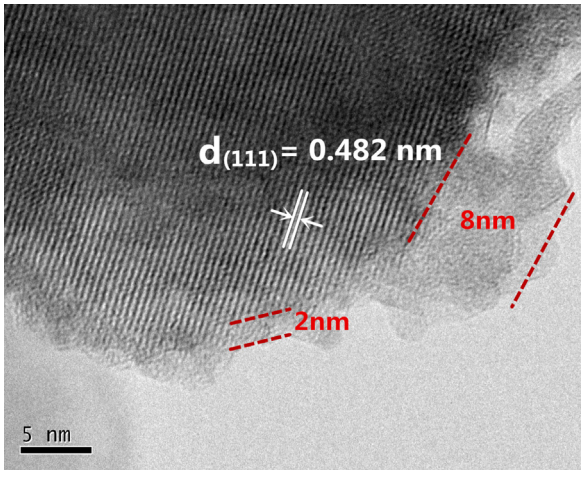

Fig. 4. HRTEM image of AlF_3-modified LTO.

The diffraction peaks can be indexed with the spinel structure of LTO with the F*d3 m* space group, indicating that AlF_3-modified process does not obviously change the crystal structure of LTO during heat treatment. For a clear observation, the peak position variation of (111) plane is magnified and shown in Fig. 1b (pure LTO shows at $2\theta = 18.3^\circ$ and AlF_3-modified LTO shows at $2\theta = 18.5^\circ$). The diffraction peak of (111) plane slightly shifts to a higher angle for AlF_3-modified LTO, which indicates that the lattice parameter of AlF_3-modified LTO is slightly smaller than that of pure LTO. This is mainly ascribed to the smaller size of Al^{3+} (0.053 nm) than Ti^{4+} (0.061 nm) and the smaller size of F^- (0.136 nm) than O^{2-} (0.140 nm). The Al^{3+} may have entered the Ti^{4+} site and the F^- may have entered the O^{2-} site, causing to form a composite of $Li_{4+x-y}Ti_{5-x}O_{12-y}F_y$ and anatase TiO_2 [44]. The peak at about 25.2 °for

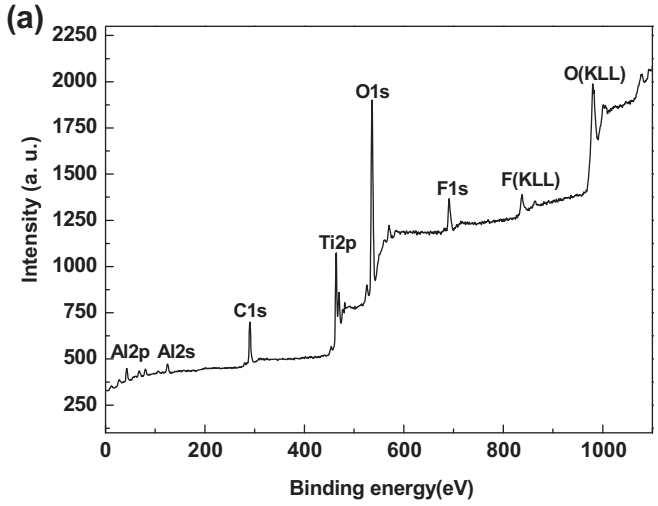

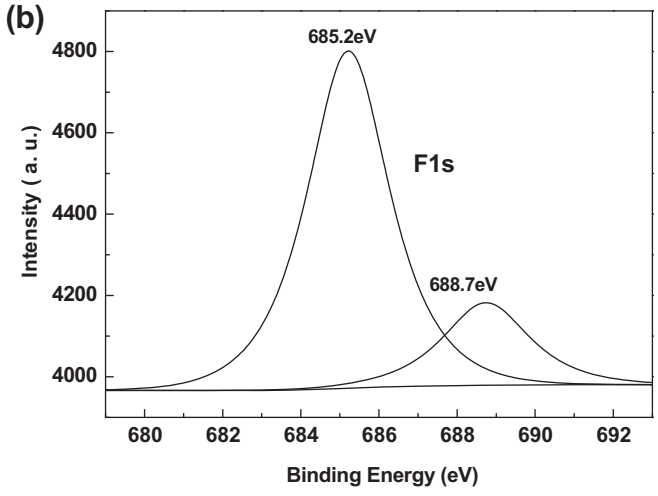

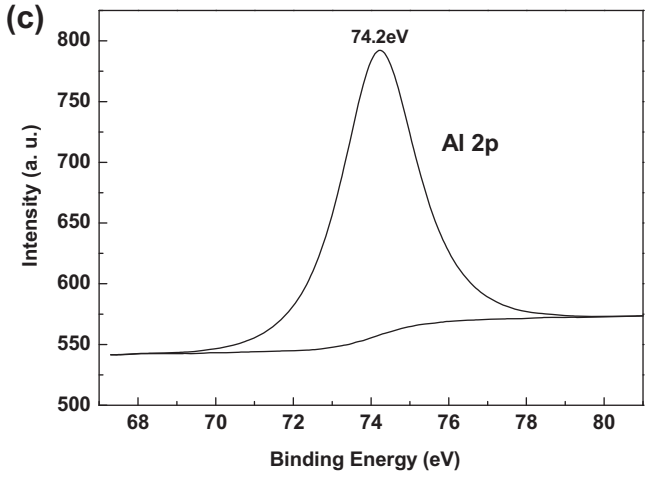

Fig. 5. (a) XPS spectrum of AlF_3-modified LTO, (b) F 1s and (c) Al 2p spectrum.

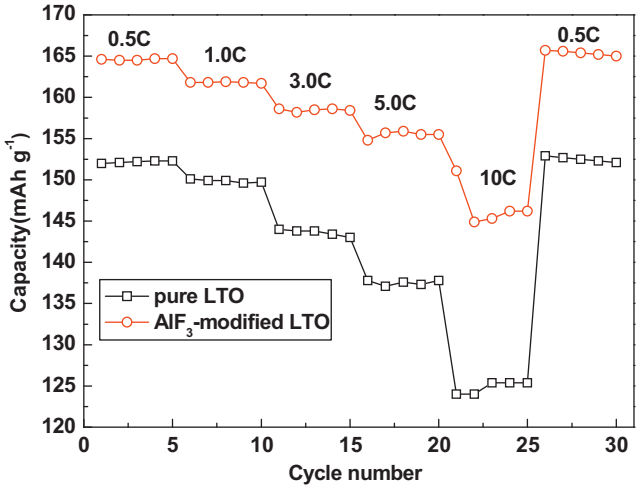

Fig. 6. Capacity retention at different C-rates (1 C = 160mAh g^{-1}) of pure LTO and AlF_3-modified LTO.

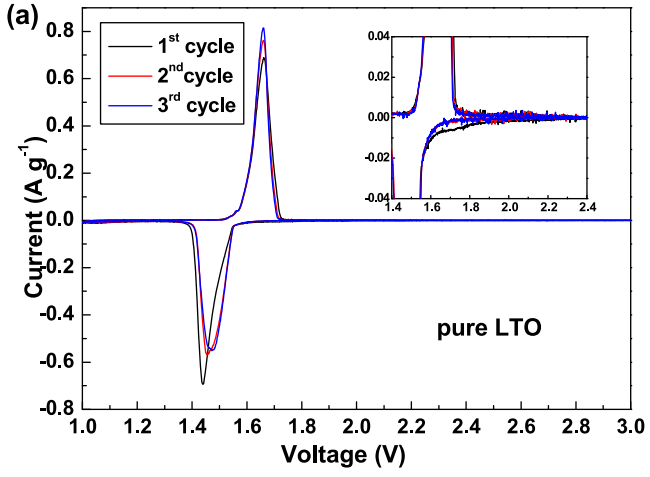

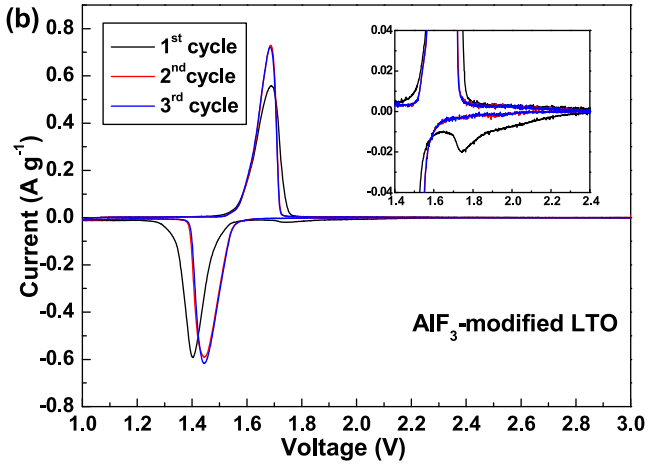

Fig. 7. Cyclic voltammetry curves of (a) pure LTO and (b) AlF_3-modified LTO.

anatase TiO_2 is hardly found in the patterns of AlF_3-modified LTO, which might be due to the fact that the formed anatase TiO_2 is too small to be detected.

Fig. 2 displays the SEM images of pure LTO and AlF_3-modified LTO. One can see that the pure LTO particles show a well-crystallized structure and smooth surface. By contrast, the AlF_3-modified LTO particles present a rough surface. From the TEM images shown in Fig. 3, the edge lines of pure LTO particles are very smooth and there is no other layer on the surface of pure LTO particles, whereas there is a thin layer on the surface of the AlF_3-modified LTO particles, demonstrating the possible existence of a thin AlF_3 layer on the surface of LTO particles after the AlF_3-modified process. HRTEM was carried out to further study the outer layer on the AlF_3 modified LTO particles, and the result is shown in Fig. 4. The lattice distance of AlF_3-modified LTO is measured to be 0.482 nm, which is very close to that of pure LTO ($d_{(111)}$ = 0.485 nm), with an error of 0.67%. It is also evident that the surface of the AlF_3-modified LTO particles is covered by a dense and non-uniform thin layer determined to be about 2 ~ 8 nm in thickness. In order to confirm the existence of AlF_3 layer on the surface of AlF_3-modified LTO, XPS measurement was conducted to determine the surface composition of AlF_3-modified LTO. Fig. 5 shows the XPS measurement of AlF_3-modified LTO. The F 1s peak at 685.2 eV and 688.7 eV observed in Fig. 5b is related to F^-, while the peak at 74.3 eV shown in Fig. 5c is associated with Al^{3+}. This indicates that the layer coating on the surface of AlF_3-modified LTO contains Al^{3+} and F^-.

Therefore, based on the above results, it can be concluded that after the AlF_3-modified process, part of the Al^{3+} and F^- have been co-doped into the bulk phase of LTO particles and the rest of the Al^{3+} and F^- form a thin AlF_3 coating layer on the surface of LTO particles.

Fig. 6 presents the rate capability of the LTO electrodes between 1.0 and 3.0 V at room temperature. The specific capacities for AlF_3-modified LTO are 164, 162, 159, 156 and 145 mAh g^{-1} at 0.5 C, 1 C, 3 C, 5 C and 10 C rate, respectively, while those for the commercial LTO are 153, 150, 147, 143 and 130 mAh g^{-1}, respectively. The results indicate that AlF_3-modified LTO show better rate capability than pure LTO.

Fig. 7 show the cyclic voltammetry curves of the pure LTO and AlF_3-modified LTO in the voltage range of 1.0 ~ 3.0 V at a scan rate of 0.1 mV s^{-1} in the first three cycles. For the AlF_3-modified LTO, there is a reduction peak shown in the 1st cycle below 1.8 V (the inset of Fig. 7b), which is ascribed to the Li^+ insertion into TiO_2 [44]. Moreover, the reduction peaks disappear from after the 1st cycle, which might be due to that the in-situ generated anatase TiO_2 is very few and unstable. The Li^+ might have intercalated into the unstable TiO_2, but could not de-intercalate from the TiO_2.

Electrochemical impedance spectroscopy (EIS) measurement of the LTO electrodes was carried out at the first cycle and half charged state, and typical Nyquist plots are given in Fig. 8. The Nyquist plots are composed of two partially overlapped and depressed semicircles in the high-frequency region. The depressed semicircles in high

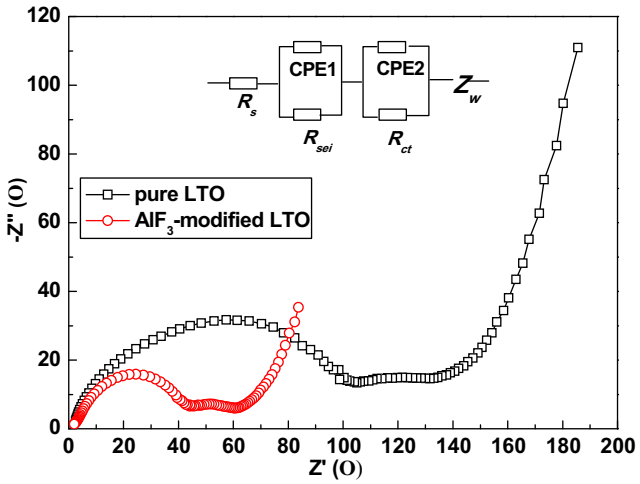

Fig. 8. Nyquist plots of pure LTO and AlF_3-modified LTO.

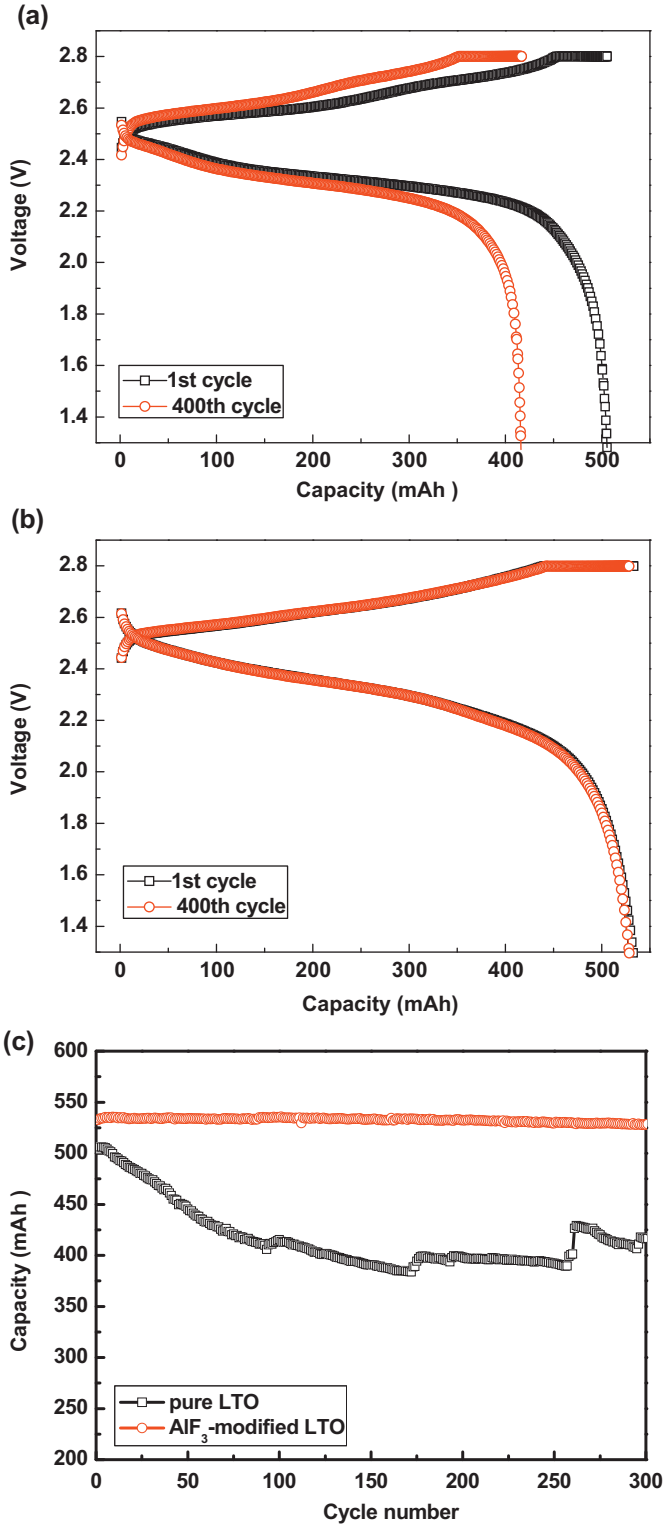

Fig. 9. Charge-discharge curves of (a) pure LTO, (b) AlF_3-modified LTO soft-packed batteries and (c) cycling stability of LMO/LTO batteries at 1 C rate.

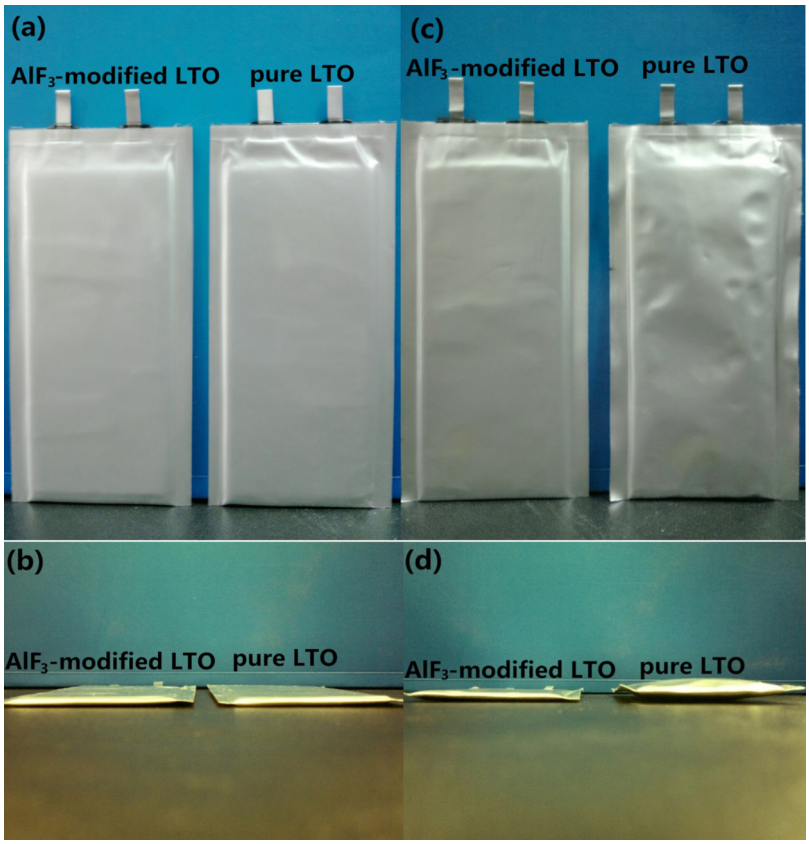

Fig. 10. Photographs of soft-packed LMO/LTO batteries (a-b) before and (c-d) after cyclic tests.

Table 1
Fitted parameters of equivalent circuit of Fig. 8.

Samples	$R_s(\Omega)$	$R_{sei}(\Omega)$	$R_{ct}(\Omega)$
pure LTO	2.5	104.1	45.2
AlF_3-modified LTO	2.0	40.3	22.5

frequency region can be attributed to the resistance of SEI film (R_{sei}). Those in middle frequency region are caused by charge-transfer resistance (R_{ct}) at the interface between electrolyte and electrode, and the sloped lines in low frequency region can be considered as the Warburg impedance (W) [19,31,45]. The values of R_s, R_{sei} and R_{ct} are obtained from the simulated data of EIS by the equivalent circuit as inserted in Fig. 8, and listed in Table 1. AlF_3-modified LTO presents relatively lower R_{ct} than pure LTO, which should be ascribed to two facts: (1) part of Al^{3+} and F^- have co-doped into the bulk phase of LTO particles, improving the electrical conductivity [44]; (2) the conductive AlF_3 coating layer is likely to enhance the electrical conductivity [43]. As a result, the improved high-rate performance of AlF_3-modified LTO could be explained both by ion doping and surface modification by conductive layer. Moreover, the R_{sei} of AlF_3-modified LTO (40.3 Ω) is obviously lower than that of pure LTO (100.1 Ω), which suggests that there is thinner SEI film formed on the AlF_3-modified LTO [31,45]. This should be due to the fact that the AlF_3 coating layer on the surface of LTO could cover the catalytic active sites and prevent the reduction decomposition of the electrolyte [31,34,45]. Therefore, AlF_3 coating layer on the surface of LTO is likely to suppress gas generation of LTO anode battery.

In order to further study the gassing behaviors of LTO anode battery, the soft-packed LMO/LTO batteries were prepared using commercial LTO or AlF_3-modified LTO as the anode, and LMO as the cathode. The soft-packed LMO/LTO batteries were charged and discharged 300 cycles between 1.3 and 2.8 V at a rate of 1 C at 25 °C. Fig. 9a-b displays the charge-discharge curves of soft-packed LMO/LTO batteries. The capacities of soft-packed LMO/LTO battery using pure LTO as the anode measured after the 1st and 300th cycles at 1 C rate are 504.1 mAh and 416.6 mAh, respectively (Fig. 9a). The soft-packed LMO/LTO battery using AlF_3-modified LTO as the anode presents much higher capacities of 532.7mAh and 528.5 mAh, respectively (Fig. 9b). Fig. 9c shows the cycling stability of soft-packed LMO/LTO batteries. The soft-packed LMO/LTO battery using AlF_3-modified LTO as the anode presents much higher cyclic stability than that using pure LTO as the anode, testament to the beneficial effect of the AlF_3 coating. Moreover, the generated gas volume of soft-packed LMO/LTO batteries is calculated by drainage method. The generated gas volume of soft-packed LMO/LTO battery using AlF_3-modified LTO as the anode (1.5 mL) is much smaller than that of soft-packed LMO/LTO battery using commercial LTO as the anode (9.2 mL). This suggests that the AlF_3 coating layer on the surface of LTO is very effective in suppressing the gassing behavior of LTO battery. Fig. 10 shows the photographs of soft-packed LMO/LTO batteries before and after cyclic tests. In particular, from Fig. 10c-d, one can see that no visible swelling occurs for the soft-packed LMO/LTO battery using AlF_3-modified LTO as the anode after cyclic test, unlike the LMO/LTO using commercial LTO as the anode.

4. Conclusion

With the purpose of suppressing the gas generation of LTO anode battery, commercial LTO was modified using AlF_3. The AlF_3-modified LTO achieved higher specific capacity and rate capability than that of the commercial LTO. It is found that for AlF_3-modified LTO, only part of Al^{3+} and F^- have co-doped into the LTO particles,

while the rest of Al^{3+} and F^- form an AlF_3 coating layer on the surface of LTO particles. The gassing behavior of the AlF_3-modified LTO anode battery was investigated for the first time. The results indicate that the AlF_3 coating layer on the surface of LTO is very effective in suppressing the gas generation of LTO battery. Therefore, using AlF_3 to modify LTO is a simple yet very effective strategy, which can both improve the high-rate charge/discharge performance of LTO and suppress the gassing behavior of LTO anode battery.

Acknowledgment

This work was carried out with financial support from the Ministry of Science and Technology of the People's Republic of China (grant no. 2011CB932604), the 973 Program (grant no.2013CB934700), and the National Natural Science Foundation of China (grant no. 51302232).

References

[1] T. Ohzuku, A. Ueda, N. Yamamoto, Zero-strain insertion material of $Li[Li_{1/3}Ti_{5/3}]O_4$ for rechargeable lithium cells, J. Electrochem. Soc. 142 (1995) 1431.
[2] K. Zaghib, M. Armand, M. Gauthier, Electrochemistry of anodes in solid-state Li-ion polymer batteries, J. Electrochem. Soc. 145 (1998) 3135.
[3] K. Amine, I. Belharouak, Z. Chen, T. Tran, H. Yumoto, N. Ota, S.T. Myung, Y.K. Sun, Nanostructured anode material for high-power battery system in electric vehicle, Adv. Mater. 22 (2010) 3052.
[4] K. Ariyoshi, T. Ohzuku, Conceptual design for 12 V lead-free accumulators for automobile and stationary applications, J. Power Sources 174 (2007) 1258.
[5] M. Imazaki, L.N. Wang, T. Kawai, K. Ariyoshi, T. Ohzuku, Examinations on 2.5 V $Li[Li_{1/3}Ti_{5/3}]O_4/Li[Li_{0.1}Al_{0.1}Mn_{1.8}]O_4$ cells at -10, 25, and 55 degrees C for the first-generation 12 V lead-free batteries, Electrochimi. Acta 56 (2011) 4576.
[6] A. Guerfi, P. Charest, K. Kinoshita, M. Perrier, K. Zaghi, Nano electronically conductive titanium-spinel as lithium ion storage negative electrode, J. Power Sources 126 (2004) 163.
[7] B.H. Li, C.P. Han, Y.B. He, C. Yang, H.D. Du, Q.H. Yang, F.Y. Kang, Facile synthesis of $Li_4Ti_5O_{12}$/C composite with super rate performance, Energy Environ. Sci. 5 (2012) 9595.
[8] A.S. Prakash, P. Manikandan, K. Ramesha, M. Sathiya, J.M. Tarascon, A.K. Shukla, Solution-combustion synthesized nanocrystalline $Li_4Ti_5O_{12}$ as high-rate performance Li-ion battery anode, Chem. Mater. 22 (2010) 2857.
[9] S.H. Yu, A. Pucci, T. Herntrich, M.G. Willinger, S.H. Baek, Y.E. Sung, N. Pinna, Surfactant-free nonaqueous synthesis of lithium titanium oxide (LTO) nanostructures for lithium ion battery applications, J. Mater. Chem. 26 (2010) 806.
[10] C.C. Li, Q.H. Li, L.B. Chen, T.H. Wang, A facile titanium glycolate precursor route to mesoporous $Au/Li_4Ti_5O_{12}$ spheres for high-rate lithium-ion batteries, ACS Appl. Mater. Interfaces. 4 (2012) 1233.
[11] J. Lim, E. Choi, V. Mathew, D. Kim, D. Ahn, J. Gim, S.H. Kang, J. Kim, Enhanced high-rate performance of $Li_4Ti_5O_{12}$ nanoparticles for rechargeable Li-ion batteries, J. Electrochem. Soc. 158 (2011) 275.
[12] H.L. Zhao, Y. Li, Z.M. Zhu, J. Lin, Z.H. Tian, R.L. Wang, Structural and electrochemical characteristics of $Li_{4-x}Al_xTi_5O_{12}$ as anode material for lithium-ion batteries, Electiochemi. Acta 53 (2008) 7079.
[13] R. Cai, S.M.J.X. Yu, B.T. Zhao, H.T. Wang, Z.P. Shao, A novel method to enhance rate performance of an Al-doped $Li_4Ti_5O_{12}$ electrode by post-synthesis treatment in liquid formaldehyde at room temperature, J. Mater. Chem. 22 (2012) 8013.
[14] E.D. Jeong, H.J. Han, O.S. Jung, M.G. Ha, C.H. Doh, M.J. Hwang, H.S. Yang, K.S. Hong, Characterizations and electrochemical performance of pure and metal-doped $Li_4Ti_5O_{12}$ for anode materials of lithium-ion batteries, Mater. Res. Bull. 47 (2012) 2847.
[15] J.P. Zhu, J.J. Zhao, H.W. Yang, G. Yang, $Li_{4-x}Mg_xTi_5O_{12}(0.05\leq x\leq 0.2)$ anode material with improved rate and electrochemical performance for Li-ion batteries, Adv. Sci. Lett. 4 (2011) 484.
[16] X. Li, M.Z. Qu, Z.L. Yu, Structural and electrochemical performances of $Li_4Ti_{5-x}Zr_xO_{12}$ as anode material for lithium-ion batteries, J. Alloys Compd. 487 (2009) 12.
[17] T.F. Yi, B. Chen, H.Y. Shen, R.S. Zhu, A.N. Zhou, H.B. Qiao, Spinel $Li_4Ti_{5-x}Zr_xO_{12}(0\leq x\leq 0.25)$ materials as high-performance anode materials for lithium-ion batteries, J. Alloys Compd. 558 (2013) 11.
[18] T.F. Yi, H.P. Liu, Y.R. Zhu, L.J. Jiang, Y. Xie, R.S. Zhu, Improving the high rate performance of $Li_4Ti_5O_{12}$ through divalent zinc substitution, J. Power Sources 215 (2012) 258.
[19] T.F. Yi, Y. Xie, L.J. Jiang, J. Shu, C.B. Yue, A.N. Zhou, M.F. Ye, Advanced electrochemical properties of Mo-doped $Li_4Ti_5O_{12}$ anode material for power lithium ion battery, RSC Adv. 2 (2012) 3541.
[20] Y.J. Bai, C. Gong, Y.X. Qi, N. Lun, J. Feng, Excellent long-term cycling stability of La-doped $Li_4Ti_5O_{12}$ anode material at high current rates, J. Mater. Chem. 22 (2012) 19054.
[21] T.F. Yi, J. Shu, Y.R. Zhu, X.D. Zhu, R.S. Zhu, A.N. Zhou, Advanced electrochemical performance of $Li_4Ti_{4.95}V_{0.05}O_{12}$ as a reversible anode material down to 0 V, J Power Sources 195 (2010) 285.
[22] B.B. Tia, H.F. Xiang, L. Zhang, H.H. Wang, Effect of Nb-doping on electrochemical stability of $Li_4Ti_5O_{12}$ discharged to 0 V, J Solid State Electrochem. 16 (2012) 205.
[23] D. Capsoni, M. Bini, V. Massarotti, P. Mustarelli, G. Chiodelli, C.B. Azzoni, M.C. Mozzati, L. Linati, S. Ferrari, Cations distribution and valence states in Mn-substituted $Li_4Ti_5O_{12}$ structure, Chem. Mater. 20 (2008) 4291.
[24] Y.L. Qi, Y.D. Huang, D.Z. Jia, S.J. Bao, Z.P. Guo, Preparation and characterization of novel spinel $Li_4Ti_5O_{12-x}Br_x$ anode materials, Electrochimi. Acta 54 (2009) 4772.
[25] Y. Wang, X.M. Liu, H. Yang, X.D. Shen, Characterization and electrochemical properties of carbon-coated $Li_4Ti_5O_{12}$ prepared by a citric acid sol-gel method, J. Alloys Compd. 509 (2011) 712.
[26] Y.H. Yin, S.Y. Li, Z.J. Fan, X.L. Ding, S.T. Yang, Synthesis of novel anode $Li_4Ti_5O_{12}$/C with PAN as carbon source and its electrochemical performance, Mater. Chem. Phys. 130 (2011) 186.
[27] G.J. Wang, J. Gao, L.J. Fu, N.H. Zhao, Y.P. Wu, T. Takamura, Preparation and characteristic of carbon-coated $Li_4Ti_5O_{12}$ anode material, J. Power Sources 174 (2007) 1109.
[28] J.P. Zhu, W. Zu, J.J. Yang, G. Yang, Q.B. Xu, Effects of Ag doping and coating on the performance of lithium ion battery material $Li_4Ti_5O_{12}$, Nanotechnol. 12 (2012) 2539.
[29] S.H. Huang, Z.Y. Wen, X.J. Zhu, X.L. Yang, Research on $Li_4Ti_5O_{12}/Cu_xO$ composite anode materials for lithium-ion batterie, J. Electrochem. Soc. 152 (2005) 1301.
[30] Y.Y. Wang, Y.J. Hao, Q.Y. Lai, J.Z. Lu, Y.D. Chen, X.Y. Ji, A new composite material $Li_4Ti_5O_{12}$-SnO_2 for lithium-ion batteries, Ionics 14 (2008) 85.
[31] J. Liu, X.F. Li, M. Cai, R. Li, X.L. Sun, Ultrathin atomic layer deposited ZrO_2 coating to enhance the electrochemical performance of $Li_4Ti_5O_{12}$ as an anode material, Electrochimi. Acta 93 (2013) 195.
[32] I. Belharouak, G.M. Koenig, T. Tan, H. Yumoto, N. Ota, K. Amine, Performance degradation and gassing of $Li_4Ti_5O_{12}/LiMn_2O_4$ lithium-ion cells, J. Electrochem. Soc. 159 (2012) 1165.
[33] K. Wu, J. Yang, Y. Zhang, C.Y. Wang, D.Y. Wang, Investigation on $Li_4Ti_5O_{12}$ batteries developed for hybrid electric vehicle, J Appl Electrochem 42 (2012) 989.
[34] A. Du Pasquier, I. Plitz, S. Menocal, G. Amatucci, A comparative study of Li-ion battery, supercapacitor and nonaqueous asymmetric hybrid devices for automotive applications, J Power Sources 115 (2003) 171.
[35] X. Lu, L. Zhao, X.Q. He, R.J. Xiao, L. Gu, Y.S. Hu, H. Li, Z.X. Wang, X.F. Duan, L.Q. Chen, J. Maier, Y. Ikuhara, Lithium storage in $Li_4Ti_5O_{12}$ spinel: The full static picture from electron microscopy, Adv. Mater. 24 (2012) 3233.
[36] Z.J. Ding, L. Zhao, L.M. Suo, Y. Jiao, S. Meng, Y.S. Hu, Z.X. Wang, L.Q. Chen, Towards understanding the effects of carbon and nitrogen-doped carbon coating on the electrochemical performance of $Li_4Ti_5O_{12}$ in lithium ion batteries: a combined experimental and theoretical study, Phys. Chem. Chem. Phys. 13 (2011) 15127.
[37] Y.B. He, B.H. Li, C. Zhang, W. Lv, C. Yang, J. Li, H.D. Du, B. Zhang, Q.H. Yang, J.K. Kim, F.Y. Kang, Gassing in $Li_4Ti_5O_{12}$-based batteries and its remedy, Sci. Rep. 2 (2012) 913.
[38] Y.K. Sun, J.M. Han, S.T. Myung, S.W. Lee, K. Aminec, Significant improvement of high voltage cycling behavior AlF_3-coated $LiCoO_2$ cathode, Electrochem. Commun. 8 (2006) 821.
[39] K.S. Lee, S.T. Myung, D. Won Kim, Y.K. Sun, AlF_3-coated $LiCoO_2$and $Li[Ni_{1/3}Co_{1/3}Mn_{1/3}]O_2$ blend composite cathode for lithium ion batteries, J. Power Sources 196 (2011) 6974.
[40] Y.K. Sun, M.J. Lee, C.S. Yoon, J. Hassoun, K. Amine, B. Scrosati, The role of AlF_3 coatings in improving electrochemical cycling of Li-enriched nickel-manganese oxide electrodes for Li-ion batteries, Adv. Mater. 24 (2012) 1192.
[41] S.H. Lee, C.S. Yoon, K. Aminec, Y.K. Sun, Improvement of long-term cycling performance of $Li[Ni_{0.8}Co_{0.15}Al_{0.05}]O_2$ by AlF_3coating, J. Power Sources 234 (2013) 201.
[42] J.M. Zheng, Z.R. Zhang, X.B. Wu, Z. Zhu, Y. Yang, The effects of AlF_3 coating on the performance of $Li[Li_{0.2}Mn_{0.54}Ni_{0.13}Co_{0.13}]O_2$ positive electrode material for lithium-ion battery, J. Electrochem. Soc. 155 (2008) 775.
[43] F. Ding, W. Xu, D. Choi, W. Wang, X.L. Li, M.H. Engelhard, X.L. Chen, Z.G. Yang, J.G. Zhang, Enhanced performance of graphite anode materials by AlF_3 coating for lithium-ion batteries, J. Mater. Chem. 22 (2012) 12745.
[44] W. Xu, X.L. Chen, W. Wang, D. Choi, F. Ding, J.M. Zheng, Z.M. Nie, Y.J. Choi, J.G. Zhang, Z.G. Yang, Simply AlF_3-treated $Li_4Ti_5O_{12}$ composite anode materials for stable and ultrahigh power lithium-ion batteries, J. Power Sources 236 (2013) 169.
[45] Y.B. Ye, F. Ning, B. Li, Q.S. Song, W. Lv, H. Du, D. Zhai, F. Su, Q.H. Yang, F. Kang, Carbon coating to suppress the reduction decomposition of electrolyte on the $Li_4Ti_5O_{12}$ electrode, J. Power Sources 202 (2012) 253.